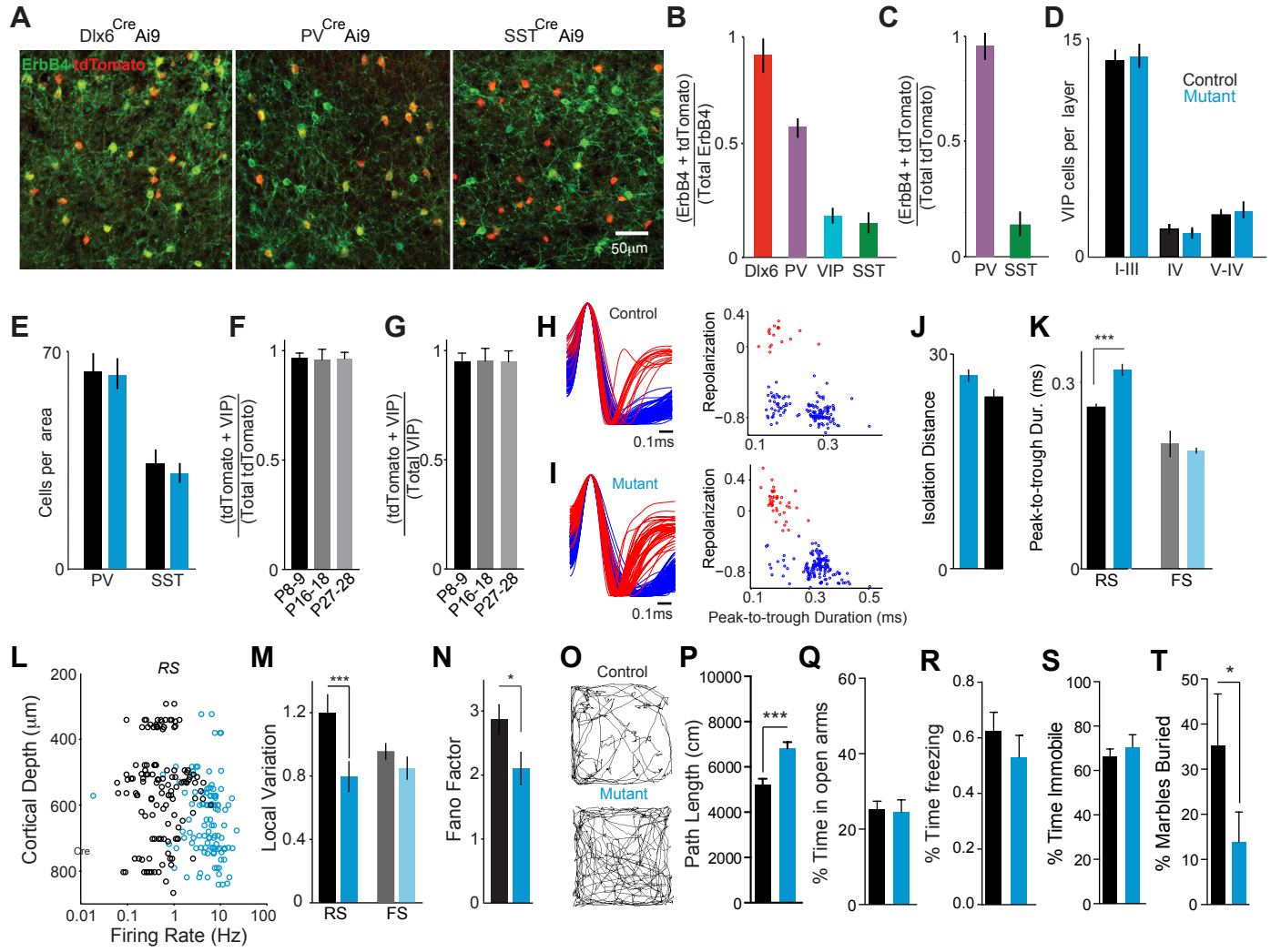

Figure S1 (Related to Figure 1). Expression of ErbB4 in interneuron populations, basic waveform and firing characteristics, and standard behavioral assays for ErbB4-VIP mutants and controls. (**A**) ErbB4 (green) and tdTomato (red) immunohistochemistry in the visual cortex (V1) of P60 Dlx6^{Cre}(pan-interneuron marker), PV^{Cre} and SST^{Cre} mice crossed to the reporter line Ai9. (**B**) ErbB4 expression in Dlx6, PV, SST, and VIP fate-mapped cells shows that the vast majority of ErbB4-expressing cells in V1 are interneurons. (**C**) PV and SST fate-mapped interneurons that express ErbB4 in the V1. Most PV interneurons, but few SST interneurons, express ErbB4. N=6 mice for each quantification. (**D**) Distribution of VIP cells per cortical layer for controls (black) and mutants (cyan). There was no effect of ErbB4 removal on VIP-IN distribution. (**E**) Distribution of PV and SST interneurons in V1, measured as cells per standard area. There was no effect of ErbB4 removal from VIP-INs on either PV or SST cell numbers. (**F**) Nearly all Cre-expressing neurons in the VIP-Cre line were co-positive for VIP at all developmental ages. (**G**) Nearly all VIP-expressing neurons in the VIP-Cre line were co-positive for Cre at all developmental ages. N = 4 control and 4 mutant mice for each quantification in panels A-G except where otherwise noted. (**H**) Left: normalized AP waveforms, aligned to AP peak. Right: peak-to-trough duration of action potentials (APs) vs. AP repolarization metric, which was defined as the value of the normalized (between -1 and +1) AP waveform at 450 ms (as in Vinck et al., 2015). We separated three clusters of waveforms in both controls and mutants using a Gaussian mixture model, as in Vinck et al. (2015). Putative RS cells can be subdivided into groups with thin and broad spikes (Haider et al., 2010, Vinck et al., 2015) that both have low firing rates in wild-type animals (Vinck et al., 2015). The distributions of RS and FS cell firing rates were largely non-overlapping in control mice (see Fig. 1). (**I**) Same as in (**H**), but for mutant mice. (**J**) Median ± s.e.m. of isolation distance for cells in mutant and control mice. (**K**) Peak-to-trough duration for RS and FS cells. RS cells in mutant mice have broader action potentials on average. Controls: 153 RS, 15 FS cells, 8 mice. Mutants: 134 RS, 32 FS cells, 8 mice. (**L**) Firing rate vs cortical depth for RS cells in control (black) and mutant (cyan) mice. (**M**) Local Variation, a measure of the irregularity of spike trains. RS, but not FS cells in mutant animals fire more regularly than those in controls. (**N**) Average Fano factor, defined as the variance of the spike count over the mean spike count, for RS cells. Controls: 153 RS, 15 FS cells, 8 mice. Mutants: 134 RS, 32 FS cells, 8 mice. (**O**) Example paths in the first five minutes of the open field assay for a control (upper) and mutant (lower). (**P**) Population quantification of total open field path length (n = 29 controls, 18 mutants). (**Q**) Time spent in the open arms of the elevated plus maze assay (n= 29 controls, 21 mutants). (**R**) Percentage of time freezing 24h after the contextual fear conditioning paradigm (n = 11 controls, 15 mutants). (**S**) Percentage of time spent immobile in the forced swim assay (n = 16 controls, 6 mutants). (**T**) Percentage of marbles buried in the marble burying assay (n = 14 controls, 6 mutants). Error bars indicate mean ± s.e.m. p* < 0.05, p**<0.01, p***<0.001.

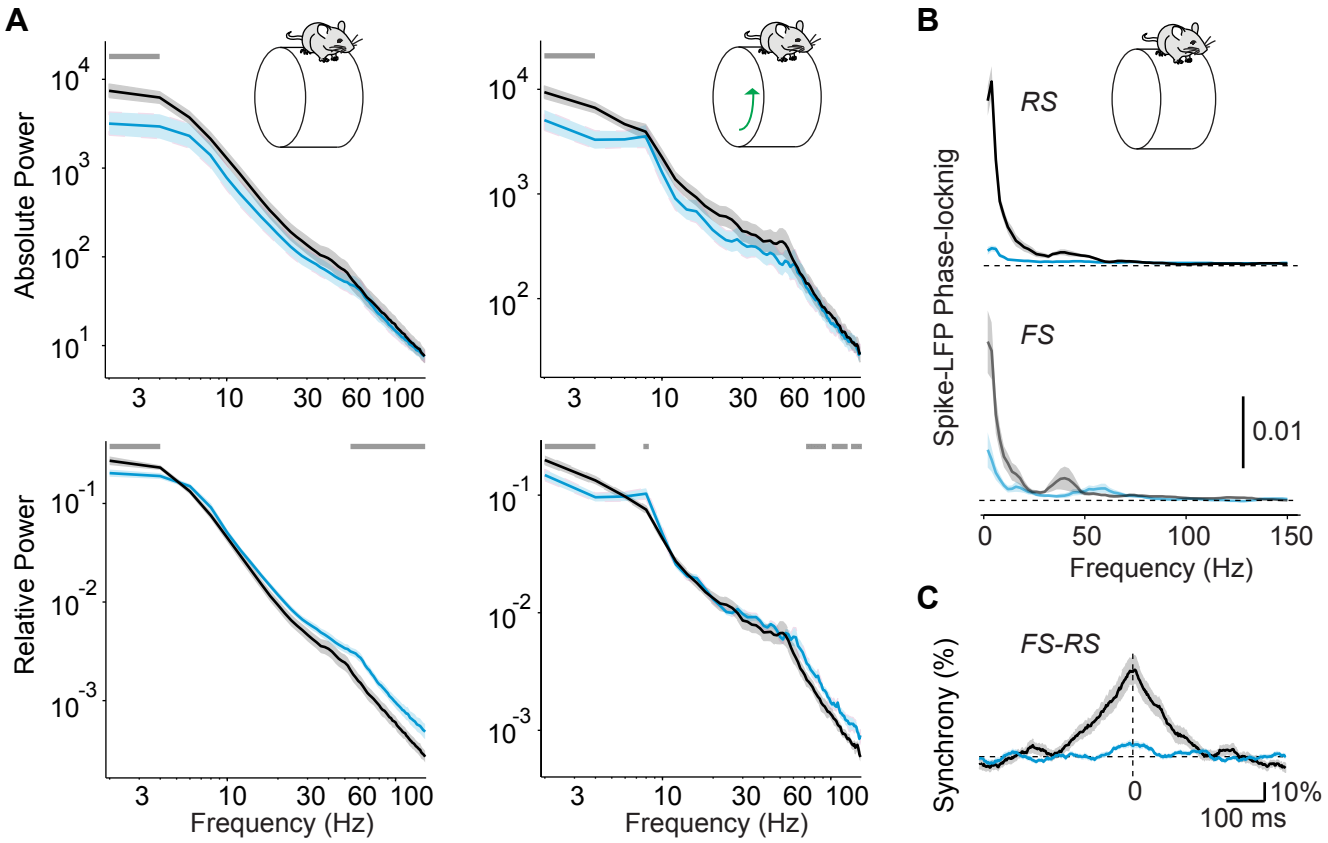

Figure S2 (Related to Figure 2). Power spectra from V1 recordings in ErbB4-VIP mutants and controls. (**A**) Upper, left: Absolute V1 LFP power for control (black) and mutant (cyan) populations during quiescence. Upper, right: Absolute LFP power spectra for control and mutant populations during locomotion, shown on a log-log scale. Lower, left: Relative LFP power spectra for control and mutant populations during quiescence. Relative power spectra were defined by dividing the power at each frequency by the summed power across frequencies. Lower, right: Relative LFP power spectra for control and mutant populations during locomotion. Controls: 21 sessions, 7 mice. Mutants: 29 sessions, 9 mice. The LFP is a complex signal that reflects thalamocortical and cortical inputs, as well as local RS and FS activity. The decrease in absolute power in low-frequency bands in mutants as compared to controls is consistent with a loss of synchrony (Figure 2), while the increase in relative high-frequency power is consistent with increased cortical firing rates in mutants (Einevoll et al 2013). Horizontal, gray bar at top indicates frequencies at which the difference between control and mutant mice was significant. (**B**) Average spike-LFP phase-locking (measured with pairwise phase consistency) during quiescence for RS (upper) and FS (lower) cells in controls (black) and mutants (cyan) (similar to Figure 2C). Both RS and FS cells in the ErbB4-VIP mutants showed decreased spike-LFP phase-locking at low- and gamma-range frequencies. Controls: 55 RS, 23 FS cells, 7 mice. Mutants: 61 RS, 23 FS, 8 mice. (**C**) Average RS-FS cell synchrony during quiescence (similar to Figure 2E). Controls: n=15 pairs in 4 mice. RS-FS Mutants: n=95 pairs in 6 mice. Controls: n=85 pairs in 8 mice.

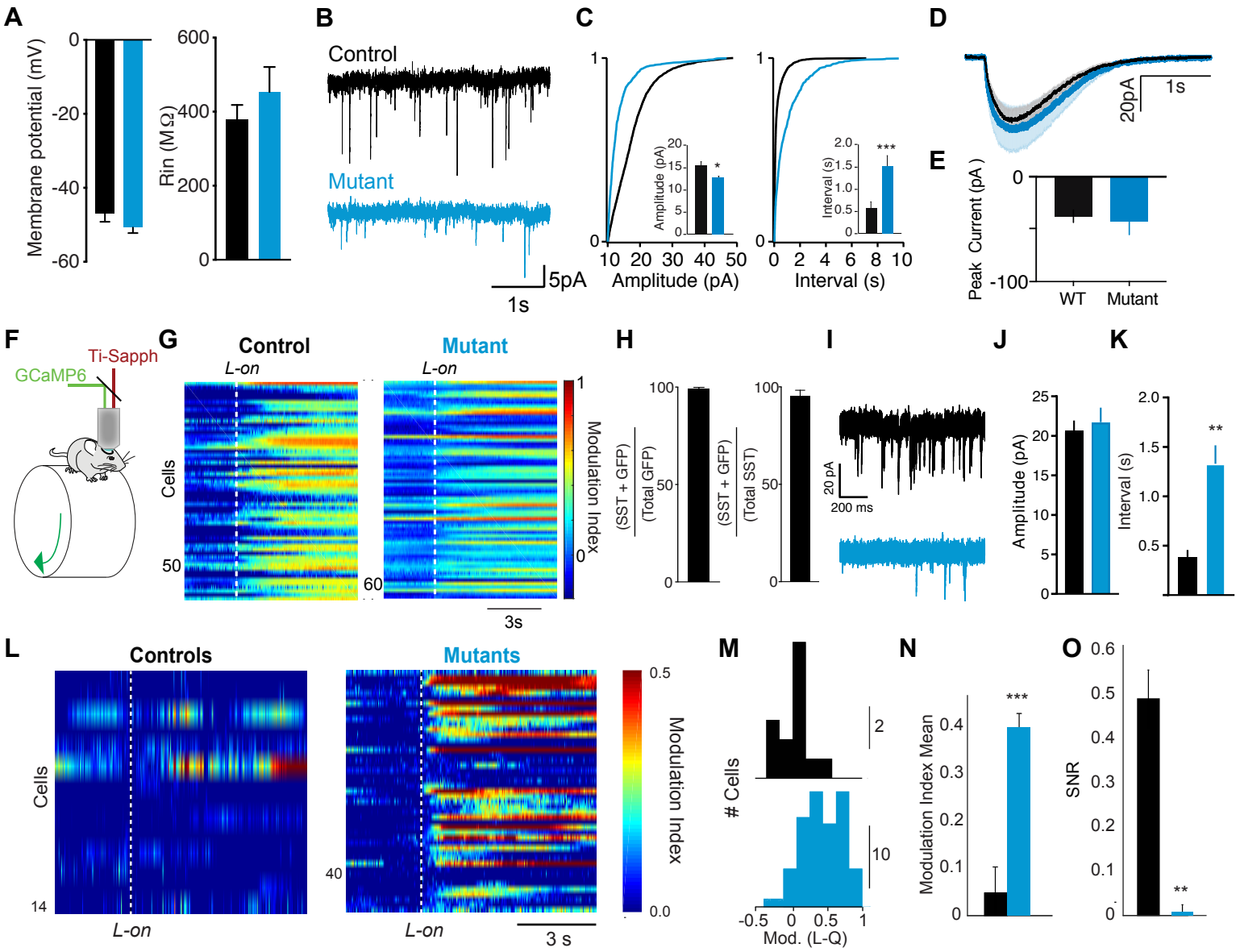

Figure S3 (Related to Figure 3). Deletion of ErbB4 reduces excitatory inputs to VIP interneurons and decreases their modulation by locomotion. (**A**) Deletion of ErbB4 did not significantly alter the membrane potential or input resistance of VIP interneurons. Controls: 6 cells, 3 mice (black). Mutants: 10 cells, 4 mice (cyan). (**B**) Example traces of miniature EPSCs (mEPSCs), a measure of glutamatergic synaptic input, recorded in VIP interneurons of control and mutant mice. (**C**) Relative to controls (black), deletion of ErbB4 (cyan) results in a significant decrease in mEPSC amplitude (left) and a significant increase in inter-event interval (right). Controls: 6 cells, 4 mice. Mutants: 12 cells, 5 mice. (**D**) Population average nAChR-mediated currents in VIP interneurons in mutant and control animals in response to puffed ACh. (**E**) Deletion of ErbB4 in VIP interneurons did not result in a change in peak nAChR current as compared to controls. Mutants: 7 cells, 5 mice. Controls: 6 cells, 4 mice. (**F**) Schematic of the *in vivo* 2-photon imaging configuration. (**G**) Modulation of the activity of each VIP interneuron around locomotion onset in two example mice. (**H**) Quantification of histology from SST-FlpO$^{+/-}$RCE$^{+/-}$animals stained with an antibody for SST. Nearly 100% of antibody-labeled SST-INs were GFP+, and nearly 100% of GFP+ SST-INs were labeled with antibody. (**I**) Miniature IPSCs, a measure of GABAergic synaptic input, recorded in SST-INs in controls (black) and mutants (cyan). (**J**) mIPSC amplitude in SST-INs in controls and mutants. (**K**) Inter-event interval for IPSCs in SST-INs in controls and mutants. (**L**) In vivo 2-photon imaging of SST-INs in controls (left; VIP-Cre$^{-/-}$ErbB4$^{f/f}$SST-FlpO$^{+/-}$) and mutants (right; VIP-Cre$^{+/-}$ErbB4$^{f/f}$SST-FlpO$^{+/-}$) measured in front of a mean-luminance gray screen around the onset of locomotion (L-on, white dotted line), measured as a modulation index (L-Q)/(L+Q). (**M**) Modulation index distributions for layer 2/3 SST-INs in controls and mutants measured in front of a mean-luminance gray screen but in the absence of visual stimuli, showing a rightward shift in the mutant population. Controls: 14 cells, 2 mice. Mutants: 90 cells, 3 mice. (**N**) Population mean modulation index values for mutants and controls. Layer 2/3 SST-INs in VIP mutants showed a significant increase in state-dependent modulation. Controls: 14 cells, 2 mice. Mutants: 90 cells, 3 mice. (**O**) Average population visual responses in SST-INs in controls and mutants, measured as signal-to-noise (SNR) during locomotion. SST-INs in VIP mutants showed a significant decrease in visual response amplitude. Controls: 14 cells, 2 mice. Mutants: 29 cells, 2 mice. Error bars indicate mean + s.e.m. *p<0.05, **p< 0.01, ***p < 0.001

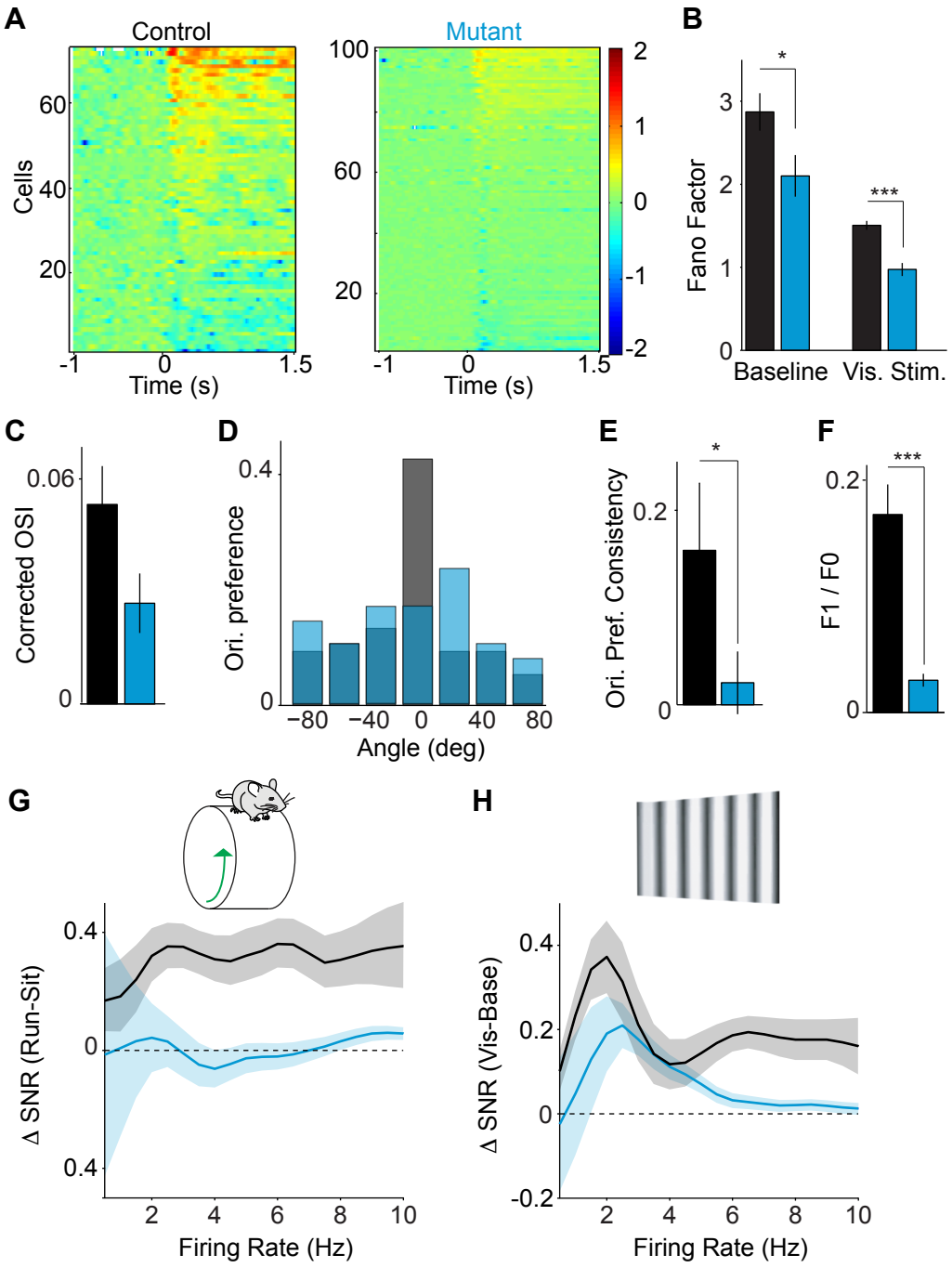

Figure S4 (Related to Figure 4). Additional quantification of visual response disruption in ErbB4-VIP mutants. (**A**) Shown for each individual RS cell the average rate modulation relative to the inter-trial interval baseline as a function of time around stimulus onset, i.e shown the rate modulation log10 FR(t) / FRbase. Left: control mice. Right: mutant mice. (**B**) Fano factor for the 30ms-500ms stimulus period and the inter-trial-interval (baseline) period. Fano factor was defined as the variance of the spike count divided by the mean of the spike count for controls (black) and mutants (cyan). (**C**) Average orientation selectivity index (OSI) with the random OSI that was obtained by shuffling trials subtracted. Corrected OSI values are higher than by chance for RS cells in both controls and mutants. (**D**) Histogram of preferred orientations across the population of RS cells for mutants and controls. (**E**) Population phase consistency of orientation preferences for controls and mutants. Controls exhibit significant clustering of preferred orientations, but mutants show no clustering. (**F**) Population average F1/F0 values for RS cells. Controls: 55 cells, 7 mice. Mutants: 61 cells, 8 mice. (**G**) Average rate modulation during early locomotion (-0.5 to 0.5s around L-on) period as compared to quiescence, as a function of firing rate for RS cells in controls and mutants.Controls: 85 cells, 5 mice. Mutants: 72 cells, 8 mice. (**H**) Average rate modulation relative to inter-trial interval baseline as a function of time around stimulus onset. Controls: 106 cells, 8 mice. Mutants: 92 cells, 7 mice. If the differences in rate modulation between control and mutant mice were explained by a ceiling effect on RS firing rate, we would expect to find no differences in rate modulation for a given firing rate bin. However, RS cells in controls showed rate modulation even at higher firing rates. Error bars and shading show s.e.m.'s. p*<0.05, p**<0.01, p***<0.001.

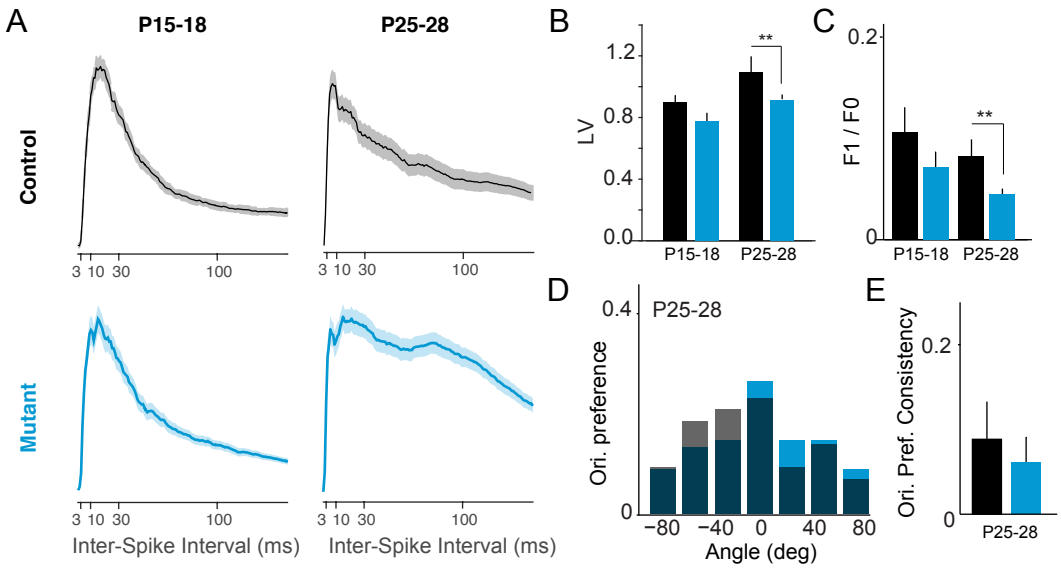

Figure S5. (Related to Fig. 5). Cortical activity in mutants and controls over post-natal development. (**A**) Inter-spike interval histograms for controls (upper, black) and mutants (lower, cyan) at P15-18 and P25-28, compare to Fig 1G for adult values. Controls: 113 cells, 4 mice (P15-18), 70 cells, 3 mice (P25-28). Mutants: 89 cells, 7 mice (P15-18), 103 cells, 4 mice (P25-28). (**B**) Population average local variance (LV) for RS cells in controls and mutants at each age, using same data set as in A. Compare to SFig. 1 for adult values. (**C**) Population average F1/F0 ratios for RS cells in controls and mutants at each age. Controls: 23 cells, 3 mice (P15-18), 43 cells, 3 mice (P25-28). Mutants: 20 cells, 3 mice (P15-18), 74 cells, 3 mice (P25-28). Compare to SFig. 4 for adult values. (**D**) Orientation preference distribution for RS cells in controls and mutants at P25-28. Controls: 43 cells, 3 mice. Mutants: 74 cells, 3 mice. (**E**) Population average orientation preference consistency for RS cells in controls and mutants at P25-28. Controls: 43 cells, 3 mice (P25-28). Mutants: 74 cells, 3 mice (P25-28). Compare to SFig. 4 for adult values. Error bars represent mean ± s.e.m.** $p < 0.01$

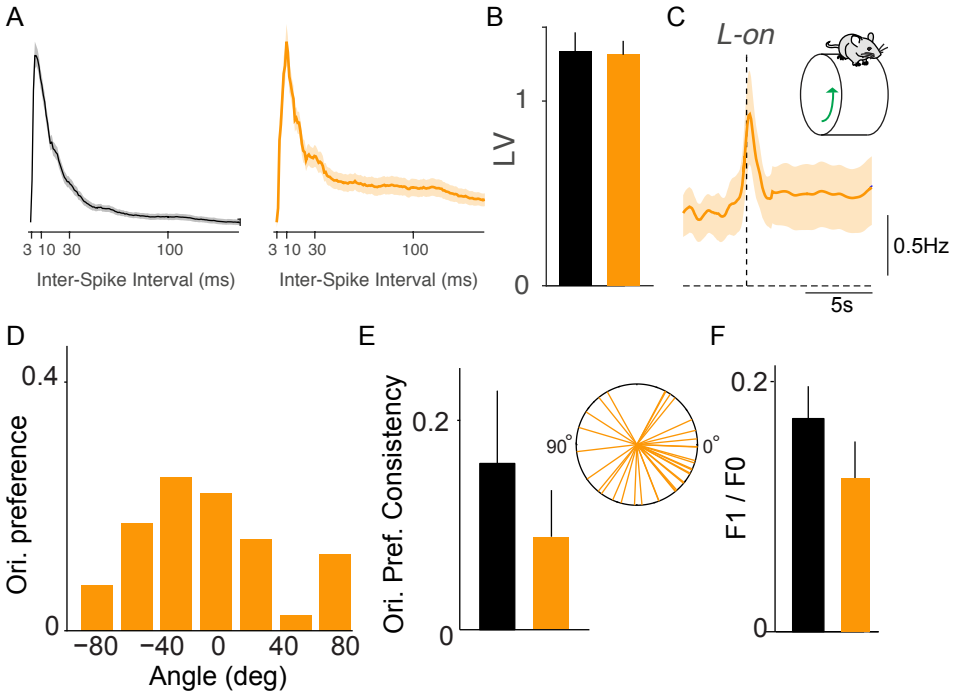

Figure S6. (Related to Fig.6) Rescue of cortical activity by viral re-expression of ErbB4 in cortical VIP-INs. (**A**) Firing rate density plots for RS cells in control (black) and re-expression (orange) animals. Controls: 153 cells, 8 mice. Rescued Mutants: 63 cells, 5 mice. (**B**) Population average local variance (LV) for RS cells in control and re-expression animals, using the same data set as in A. (**C**) Average firing rate of RS cells around the time of locomotion onset (L-on, dotted line) showing state-dependent rate modulation in re-expression animals. Rescued Mutants: 63 cells, 5 mice. (**D**) Distribution of orientation preference in RS cells in re-expression animals, using the same data set as in C. (**E**) *Left*: Population average orientation preference consistency in controls and re-expression animals, using the same data set as in C and D. *Right*: Orientation preference of each individual cell. (**F**) Population average F1/F0 ratio for RS cells in controls and re-expression animals. Controls: 106 cells, 8 mice. Rescued Mutants: 42 cells, 5 mice.

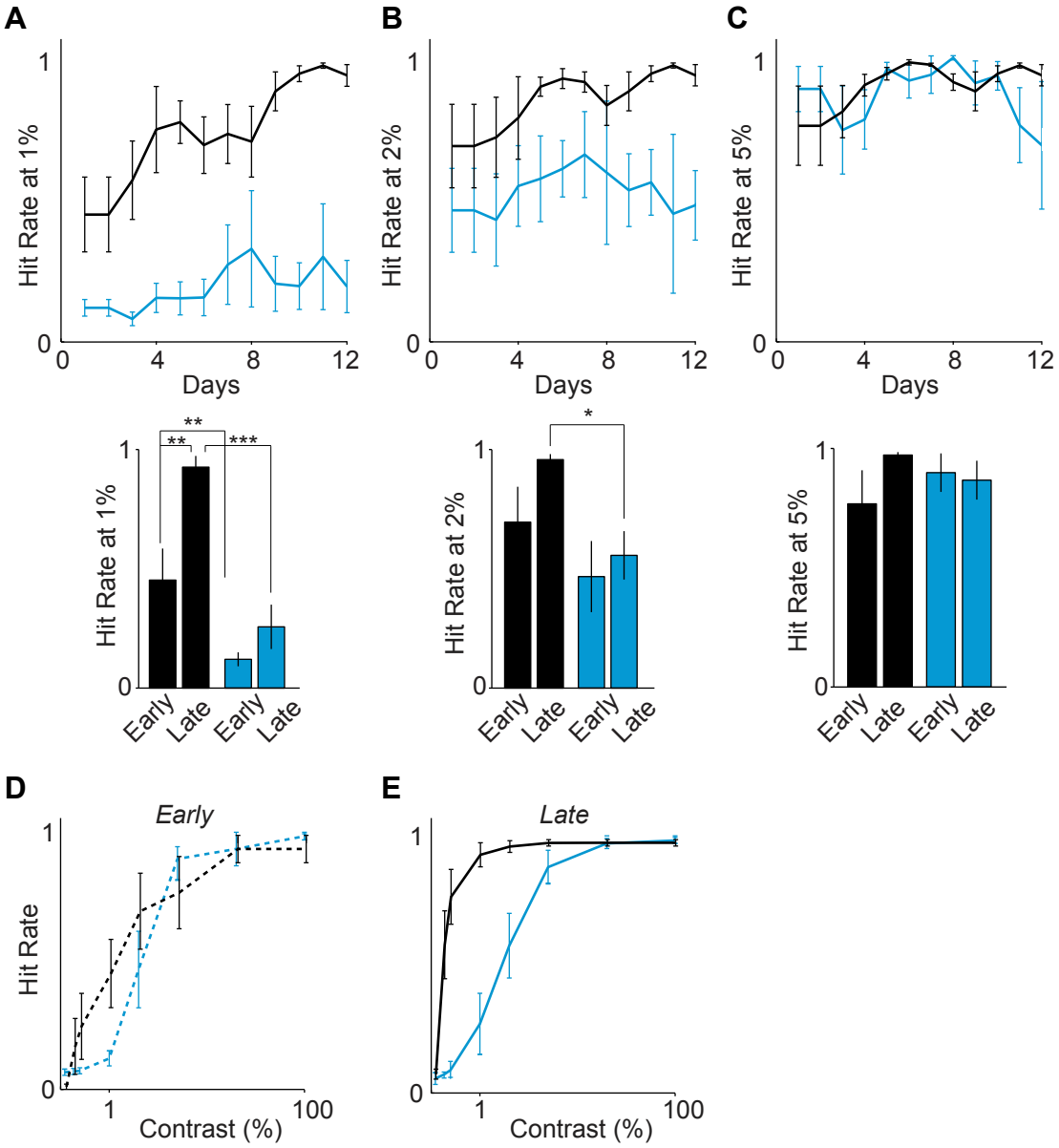

Figure S7 (Related to Figure 7) Visual task performance for control (black) and mutant (cyan) animals. (**A-C**)Top: Hit rates for 1% (**A**), 2% (**B**), and 5% (**C**) contrast stimuli over a period of two weeks. Bottom: Quantification of initial (Early) vs final (Late) performance of controls and mutants for each stimulus contrast level (similar to Figure 4K). (**D**) Psychophysical performance curves for both groups during the initial two training days. The initial psychophysical curves for mutants and controls were not significantly different except at the 1% level. (**E**) Performance curves for both groups during the final two training days. Whereas the controls showed learning, evident in the leftward shift of their performance curve between Early and Late training sessions, the mutant curve did not shift leftward over the two-week training period. Controls: 4 mice. Mutants: 4 mice. Error bars show s.e.m.'s. p*<0.05, p**<0.01, p***<0.001.